Reliability of Gas Insulated System under Electric Field Stress with Optimal Design of FGM Post Type Spacer

Akanksha Mishra [1], G. V. Nagesh Kumar[2*], D. Deepak Chowdary[3] and B. Sravana Kumar[4]

•

[1]Department of Electrical and Electronics Engineering, Vignan's Institute of Engineering for Women, Visakhapatnam, India; misakanksha@gmail.com
[2]Department of Electrical and Electronics Engineering, JNTUA CE Pulivendula, A.P, India; drgvnk14@gmail.com
[3]Department of Electrical and Electronics Engineering, Dr. L Bullayya College of Engineering, A.P, India; duvvada27@gmail.com
[4]Department of Electrical and Electronics Engineering, GITAM University, Visakhapatnam, A.P, India; sravanbali@gmail.com
*Corresponding Author

Abstract

Gas Insulated Substation (GIS) is essential for the transmission and control of power both in AC and DC electrical systems. Functionally Graded Material (FGM) technology is widely used for the design of the spacer material in the GIS to reduce the electric stress in the system. Optimal designing of the material of the spacer gradings with a particular attention to the number of gradings may prove to be very useful in reduction of the stress in the GIS at an effective cost. This paper deals with the design and development of an optimal dielectric material for the functionally graded material (FGM) spacer in a GIS. A novel optimization method has been proposed which is used for the optimization of the conductor material and the FGM epoxy spacer. The optimal value for each grading of functionally graded material spacer is determined by the proposed method. A dual-objective function is chosen for the optimization problem. The objective of the problem is to minimize the maximum field stress in addition to the standard deviation in the electric field. A post type spacer has been considered for the study. Initially, the optimization of the dielectric material is done only for 4 gradings. Gradually, the number of gradings in the FGM-spacer is increased to determine the optimal number of gradings suitable for the design.

Keywords: HVDC, Gas Insulated Substation, Functionally Graded Material, Optimization

I. Introduction

In the modern industrial world, electric power systems may easily be designated as the backbone of the world economy. A reliable power system is therefore a basic necessity in the present century. The ever-increasing load on the transmission system makes the goal rather difficult to be achieved. The privatization of power industry and rapid industrialization has increased the rapid changes in the power exchanges which may cause further instability in the transmission systems. The need for the electric power systems to become more compact and robust is at a constant rise.

The precedence of HVDC over HVAC transmission system for long distance has been established over time. Hence, the improvement of the performance and reliability of the HVDC systems is a focus of many recent researches. GIS has been associated with a considerable number of power system disturbances and failures. Hence improvement in the performance of the GIS plays an important role in increasing the reliability and stability of the power system. A lot of research is being conducted on the design aspects of HVDC power systems to improve its robustness and reliability. Wang et al [1] have proposed a method for charge dissipation from a GIS without opening the tank. Richard et al [2] have designed an efficient insulated bus pipe for shipboard applications. Sridhar et al [3] have estimated the power loss in a 420KV AC GIB by finite element method in 2-dimension. Riechert [4] has proposed the design of a compact gas Insulated System with reduced footprint on the environment. Volpov et al [5] has analyzed and formulated the SF6 spacer design for both HVAC and DC under time-varying and impulse operating conditions. Kosse et al [6] performed the design and testing for compact DC-GIS at 550 KV. The platform size of the system is expected to reduce by 10% by opting for modular designing method. Electric field stress in the power systems is the crucial factor that determines the consistency and robustness of the GIS. It has been established that the most serious distortion of electric field in a GIS occurs at the triple junction [7].

Sayed et al [8] have calculated electric field stress for different spacer types in the bus duct. An insulation compounding scheme has been proposed to reduce the flashover and stress in the AC and DC systems [9]. Zhang et al [10] have proposed the design of basin type insulators for an HVDC GIS to reduce the stress and flashover at the weak links. Researchers have studied and presented the advantage of an FGM spacer design on the electric field distribution in an GIS [11]. The effectiveness of the design has been evaluated for a multi-particle contamination [12]. Kurimoto et al [13] proposed a U-shaped distribution of ε-FGM spacer for efficient reduction in electric stress. Adari et al [14] proposed an FGM cone type spacer and studied its effectiveness under delaminated condition.

Many researchers have proposed the use of FGM post type spacer as it is effective in reduction of electric filed stress and at the same time its simple design makes it easy to manufacture and cost effective. It is very effective in reducing the field stress at the triple junction even under a protrusion and depression condition [15,16]. Ten gradings of equal dimensions have been used in the spacer and the dielectric coefficient of the material has been designated in an increasing order. Naik et al. [17] have used a di-post FGM spacer which has been found very effective in reduction of the electric field stress. The advantageous position of the spacer due to its simple design has been cited. Metwally [18] has compared the design of disc-type, conical-shaped and the post type spacer. In this work it has been cited that while post type spacer is effective in reducing the electric field stress, inclusion of metal cavities in the design limits the flexibility of the design and limits the manufacturing cost of the spacer.

In all the above methods, it has been proposed to vary the dielectric strength of the FGM-spacer in a specific pattern for various spacer designs. However, the researchers have not concentrated on the optimization aspect of the design. The proposed designs although effective may not be the optimal solution for the problem. Recently, researchers have proposed the use of optimization methods for the optimization of the ε-FGM spacer design. Qasim etal. [19] has proposed the use of PSO for the optimization of the FGM-spacer. Talaat etal. [20] have optimized the dielectric material for a cone shaped spacer using COMSOL-live link. A U-shaped permittivity distribution has been preferred in the design. Although some research has been conducted on the optimization of the FGM-spacer. In the above works, the area of research has been limited to the optimization of the FGM-material only for a fixed number of gradings. Hence, there is a scope for further research in the design of FGM spacer, to be able to qualify the GIS as properly optimized. A detailed study to determine the number of gradings and the appropriate dimensions of the same is

necessary. The number and dimensions of the gradings may vary as per requirement based on the electric field strength in the zone. Also, the determination of the dielectric coefficient for each grading should be done very precisely to be able to provide an optimal solution to the problem.

In this paper, an optimization algorithm has been proposed for the GIS. Dual objectives have been chosen for the optimization, namely, reduction of the maximum electric field and the standard deviation in the field stress with equal weightage. The FGM-spacer material has been optimized for 4 gradings initially. The detailed results are observed. Progressively, the number of gradings is increased in the high stress zones and the optimization process is repeated. The process is continued until an increase in the number of gradings improves the value of the objective function. Since, the gradings have been designed as per requirement; they may not be of equal dimensions. At the same time, since the number of gradings is as per optimization requirements, so the cost of extra gradings is avoided. The results to verify the proposed methodology have been presented and analyzed in detail.

II. Mathematical Modelling of HVDC GIS

The distribution of electric field intensity, E can be determined from the Poisson's Equation [21].

$$E = -\nabla V \tag{1}$$

Where, V is the electric Potential applied in Volt (V)

The electric flux density D in the distributed area is given by

$$D = \varepsilon_0 \varepsilon_r E(C/m^2) \tag{2}$$

where, $\varepsilon_0 = 8.854 \times 10^{-12}(F/m)$ and ε_r = relative dielectric strength of the medium

We know,

$$\nabla . D = \rho_v \tag{3}$$

ρ_v = volume charge density in C/m^3

$$-\nabla.(\varepsilon_0 \varepsilon_r (\nabla V)) = \rho_v \tag{4}$$

Assuming there are no free charges, $\rho_v = 0$, we have

$$\nabla^2 V = 0 \tag{5}$$

The finite element method can be used to analyze different constructions of the GIB. In FEM, the electrostatic energy in the given space can be minimized by the following analysis.

$$W = \frac{1}{2}\int_v \varepsilon E^2 dv \tag{6}$$

In 3-D dimensions the electrostatic energy in terms of electrical potential is given by-

$$W = \frac{1}{2}\int_v \left[\varepsilon_r \left(\frac{\partial V}{\partial r}\right)^2 + \varepsilon_\phi \left(\frac{\partial V}{\partial \phi}\right)^2 + \varepsilon_z \left(\frac{\partial V}{\partial z}\right)^2 \right] ds \tag{7}$$

Where, $\boldsymbol{\varepsilon_r}$, $\boldsymbol{\varepsilon_\emptyset}$ and $\boldsymbol{\varepsilon_z}$ are the r, ϕ, z- components of the dielectric constant.

In this case, $\left(\frac{\partial V}{\partial \emptyset}\right) = \mathbf{0}$. For a 2D simulation,

$$W = \frac{1}{2}\int_v \left[\varepsilon_r \left(\frac{\partial V}{\partial r}\right)^2 + \varepsilon_z \left(\frac{\partial V}{\partial z}\right)^2 \right] ds \tag{8}$$

Where, s is the bounded surface.

After further simplification,

$$\left\lfloor \frac{\partial W'}{\partial V_1} \right\rfloor ---- \left\lfloor \frac{\partial W'}{\partial V_n} \right\rfloor = 0 \tag{9}$$

$\frac{\partial W'}{\partial V}$ should be calculated at every dielectric constant domain.

III. Proposed Objective Function for the Design of the Spacer Material

When the spacer is inserted in the system, the electric field distribution becomes non-uniform. It is maximum at the junctions. A multi-objective function is chosen for optimization of spacer material.

I. Minimization of Electric Field

The electric stress distribution in the bus duct is non-uniform. It is highest at the junction of the spacer, SF6 gas and the outer coating. The objective is to reduce the maximum stress incurred by a GIS in order to reduce the occurrences of localized heating.

$$F_1(\varepsilon_i) = Max\left(E_i(\varepsilon_i)\right)\ V/m \tag{10}$$

Let,

$$Objective\ 1 = Min\ \left(F_1(\varepsilon_i)\right)$$

where, Max(E_i) is the maximum electric field for the material ε_i for each polygon of the spacer. The objective of the optimization is to choose ε of the spacer material such that the peak value electric field in the system is minimized.

Constraints:

The material of the spacer can be varied within upper and lower bounds.

$$\varepsilon_{i\,min} < \varepsilon_i < \varepsilon_{i\,max} \tag{11}$$

II. Uniform Electric Field distribution

The non-uniformity in the distribution of electric stress leads to the creation of local hot spots. To make the field distribution uniform, the standard deviation of the electric field in the system is minimized.

$$F_2(\varepsilon_i) = Min(\sigma(\varepsilon_i)) \tag{12}$$

$$\sigma(\varepsilon_i) = \sqrt{\frac{\sum_{i=1}^{n}(E_j - \mu)^2}{N}}\ V/m \tag{13}$$

E_j is the electric field at the nodes.

where, N = No. of samples

No. of samples is chosen such that the distance between neighboring samples is less than d_{max}

$$N:\ d_{min} < d < d_{max}$$

The multi-objective function is given by-

$$\min(F(\varepsilon_i)) = w_1 \times F_1(\varepsilon_i) + w_2 \times F_2(\varepsilon_i) \tag{14}$$

$$w_1 + w_2 = 1 \tag{15}$$

w_1 and w_2 are chosen such that $w_1 \times F_1(\varepsilon_i) \approx w_2 \times F_2(\varepsilon_i)$. Thus, equal weightage is given to both the objectives.

IV. Optimization of Dielectric Material of FGM Spacer

A reliable algorithm for optimization of the GIB is developed in this research paper. The flowchart for the proposed optimization algorithm is shown in Fig. 1. The flowchart explains the process of optimization of the dielectric material of each polygon of the post type spacer.

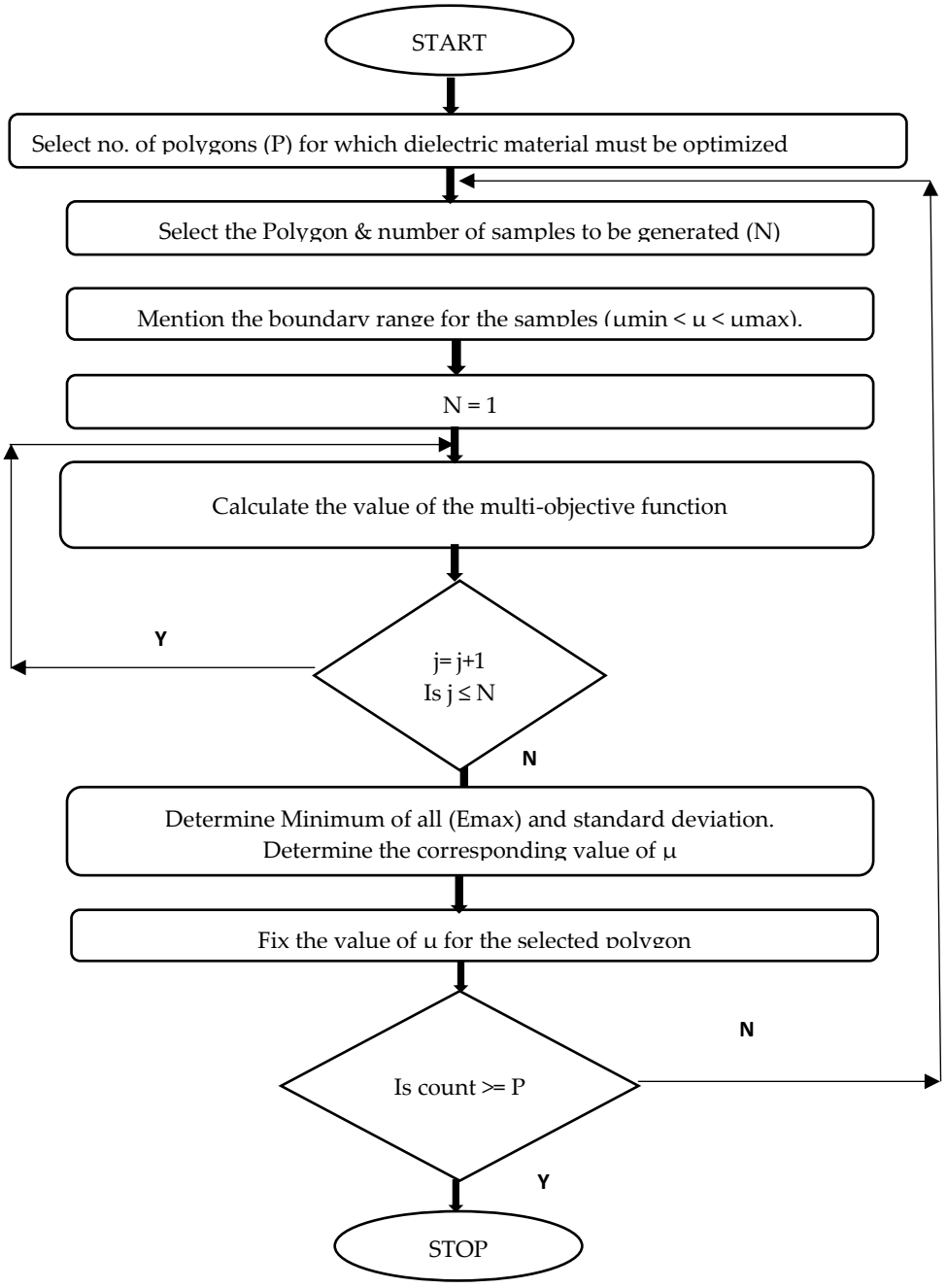

Figure 1: Flowchart depicting the optimization process for GIB post type spacer

The procedure for optimization of the spacer material is mentioned in the steps mentioned below-

Step-1 Install the post-type spacer in the GIS and optimize the dielectric strength of the material for the given multi-objective function (Fig. 1).

Step-2 Provide 4 gradings in the spacer and follow the procedure mentioned in the previous step to optimize the material of each grading.

Step-3 Increase the gradings to 6. Optimize the grading material and compare the value of the parameters and the objective function with the previous case.

Step-4 If a considerable improvement is noticed repeat the step for 8 gradings else GOTO Step-7.

Step-5 The location of the grading is chosen as per the electric field distribution in the various zones of the FGM-spacer. The zone under higher electric stress is graded into smaller zones for further optimization.

Step-6 Compare and analyze the results to obtain the final design of the FGM-Spacer.

Step-7 End Process.

III. Results

A HVDC GIS is considered for the study. The radius of the outer enclosure is 56 mm. The conductor radius is 20.4mm. The insulating medium is SF6 gas with dielectric constant of 1.06. A copper conductor is chosen for the study, with a dielectric constant of 1. The voltage applied to the conductor in this study is 1V. The values for the other voltages can be taken proportionately. The aim of the research is to develop an optimal Post-type FGM spacer for a HVDC GIS. A bi-objective function, consisting of minimization of the electric stress and the stress deviation is chosen for the optimization problem. COMSOL software has been used for the design while MATLAB software has been used for the optimization of the design.

I. Design of 4G- FGM Spacer

After the conductor radius has been optimized, the study focuses on the design of an optimal FGM post-type spacer model. Then, a post-type spacer is designed for the system. Initially, the FGM spacer has been graded into 4 equal layers, each of approximately 9mm as shown in Table 1. The material of each of the gradings of the spacer were optimized. Fig. 2 shows a sample of the optimization result for the 4^{th} grading of the spacer material. It is observed that the objective function has the minimum value at $\varepsilon = 4$. Hence, the value has been chosen for the design. Similarly, the optimization has been performed for each of the gradings of the spacer. The distribution of permittivity in the FGM spacer has been shown in Fig. 3. It is observed that the permittivity in the first grading is 4.4 while the other three gradings have a permittivity of 4 for optimal operation. The surface plots for voltage and the electric field stress distribution are shown in Fig. 4 and 5 respectively. Fig. 6 shows the line plot for the stress distribution in the FGM-spacer.

Table 1: *Permittivity distribution in 4-G FGM Spacer*

Grading No.	Distance from the Outer enclosure (mm)	Permittivity of the FGM gradings
1	0-9	4.4
2	9-18	4
3	18-27	4
4	27-36	4

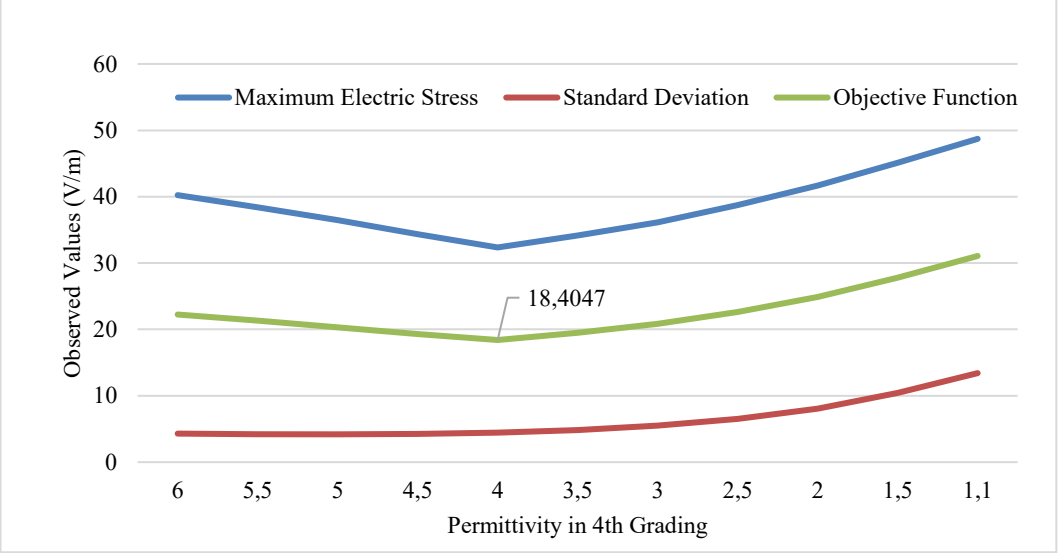

Figure 2: *Distribution of Objective function, Maximum Stress, and Standard Deviation vs permittivity for the 4th Grading of 4G-FGM Spacer*

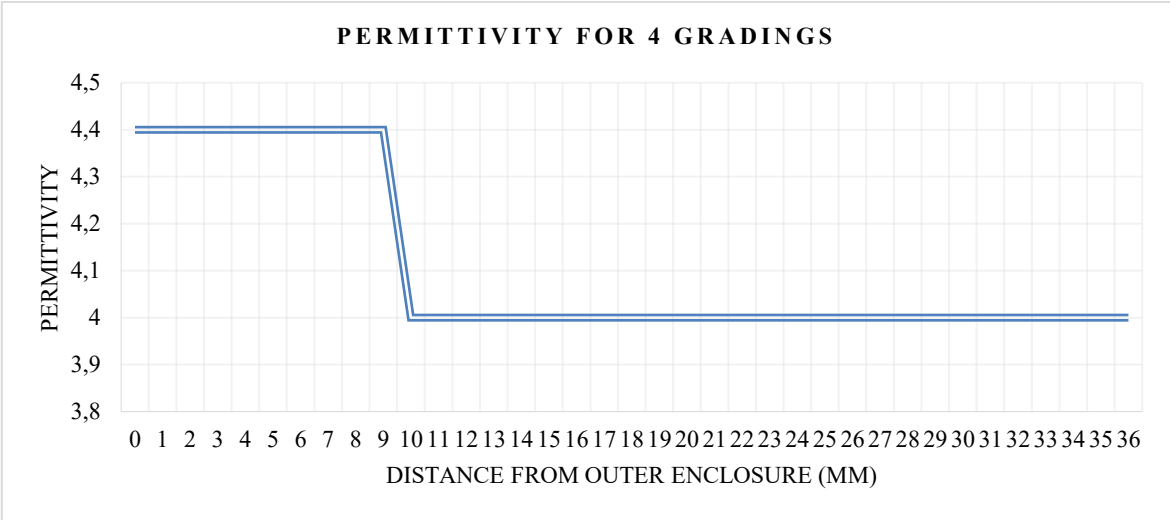

Figure 3: *Distribution of Permittivity in a 4-G FGM Spacer*

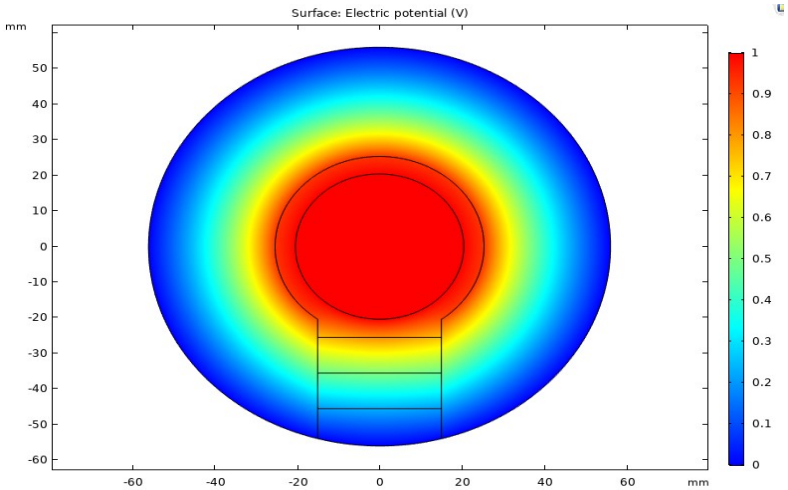

Figure 4: *Electric Potential Distribution for 4-G FGM Post Type Spacer*

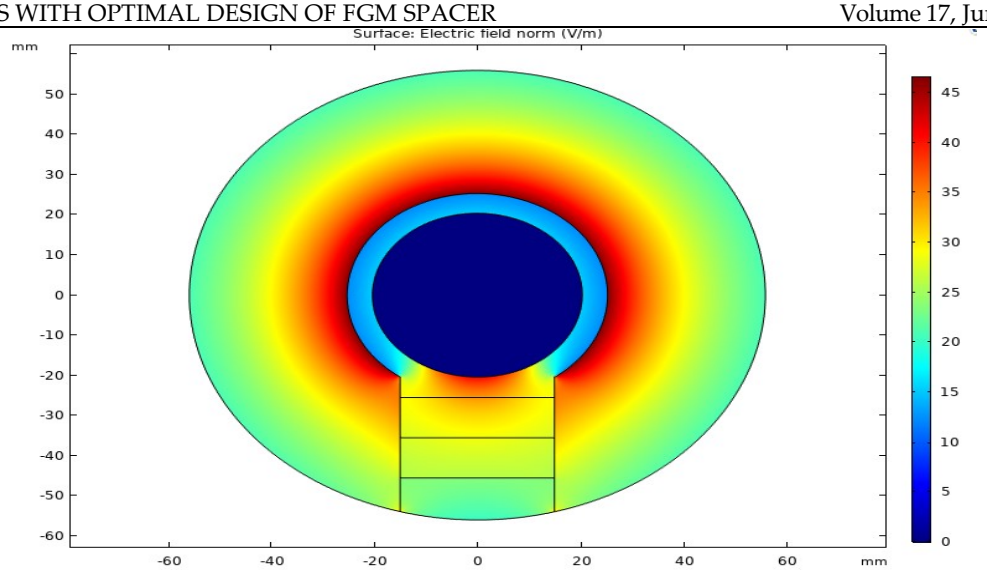

Figure 5: *Electric Field Stress Distribution Surface Plot for 4-G FGM Post Type Spacer*

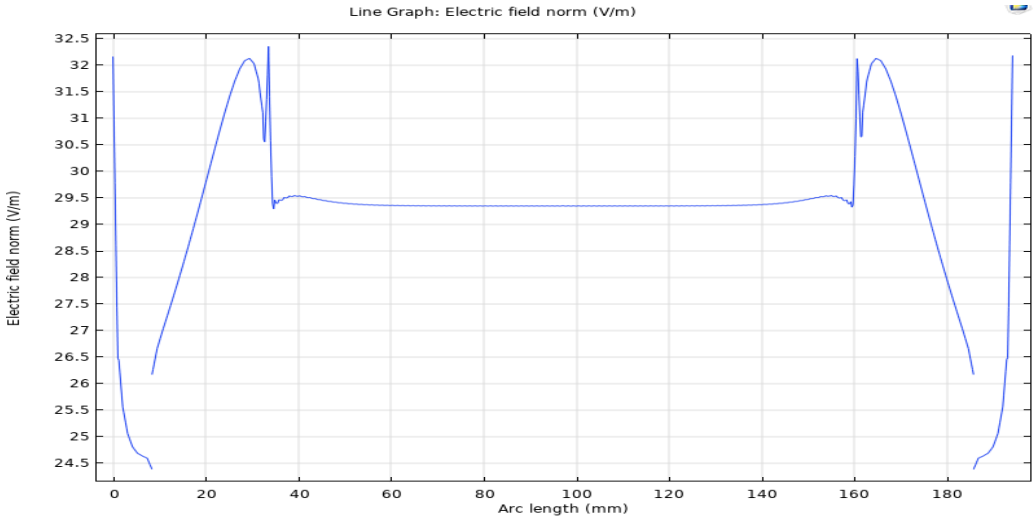

Figure 6: *Electric Field Stress Distribution Line Plot for 4-G FGM Post Type Spacer*

II. Design of 6G FGM Spacer

In a 4G FGM spacer, it is observed that the stress in grading 3 and 4 is much higher in comparison to grading 1 and 2. Hence, the layers 3 and 4 are subdivided into two more layers. The distribution of gradings with respect to distance is shown in Table 2.

Table 2: *Permittivity distribution in 6G FGM Spacer*

Grading No.	Distance from the Outer enclosure (mm)	Permittivity of the FGM gradings
1	0-9	4.8
2	9-18	3.8
3	18-22.5	3.7
4	22.5-27	4.1
5	27-31.5	4.1
6	31.5-36	3.6

The optimization of the permittivity for the 6G spacer material is performed for the chosen objective function. Fig. 7 shows the variation of objective function for various values of permittivity for the 6th grading in the 6G- FGM spacer.

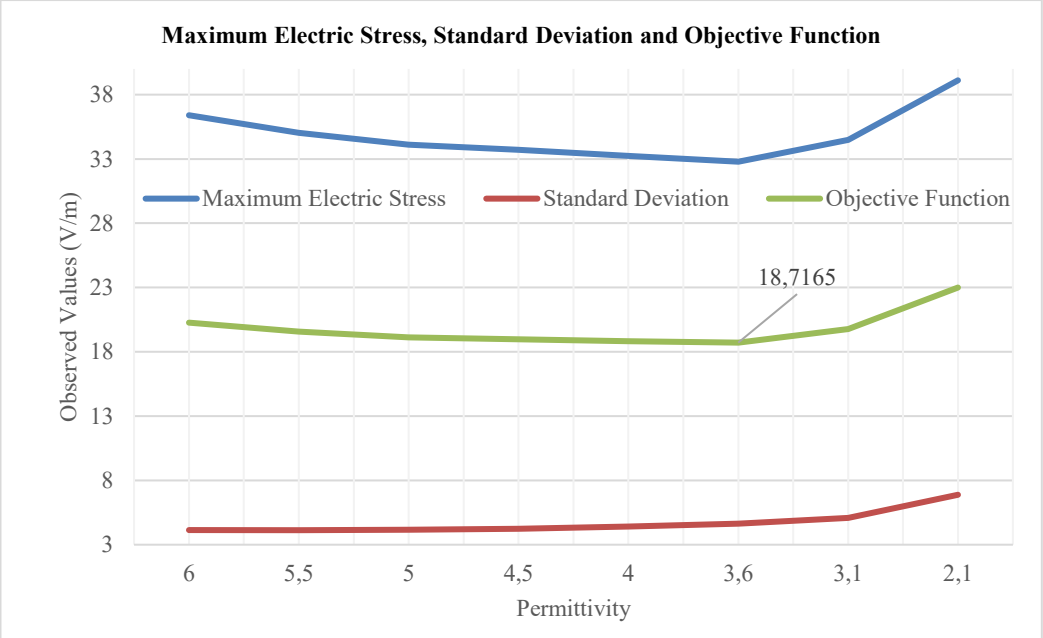

Figure 7: *Distribution of Objective function, Maximum Stress, and Standard Deviation vs permittivity for the 6th Grading of 6G-FGM Spacer*

The optimal permittivity distribution for a 6G-FGM spacer is shown in Fig. 8.

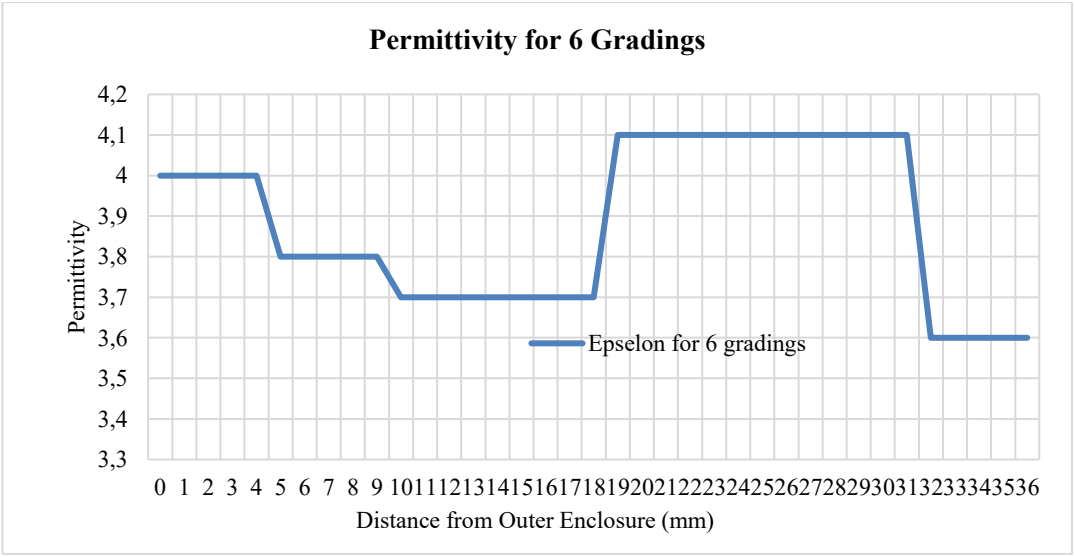

Figure 8: *Distribution of Permittivity in a 6G-FGM Spacer*

The surface plots for electric potential and electric stress for a 6G-FGM post type spacer are shown in Fig. 9 and 10 respectively. Fig. 11 shows the line plot for distribution of stress vs arc length.

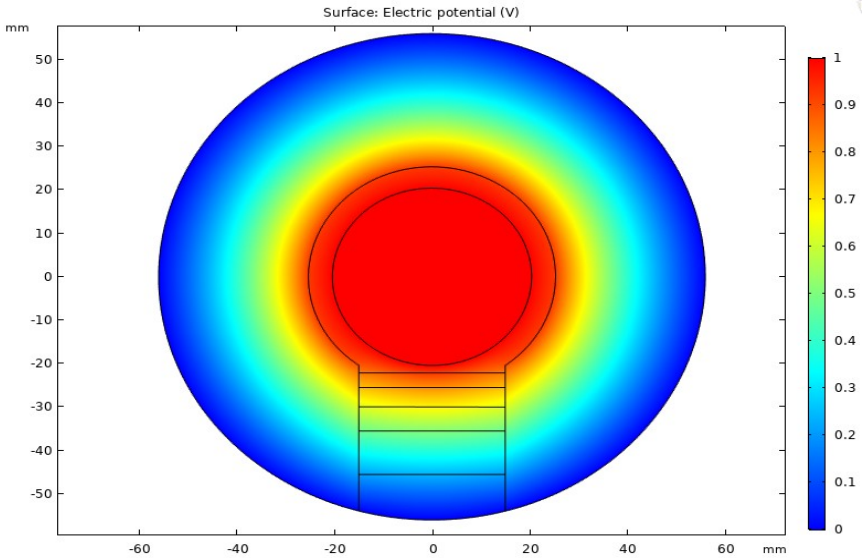

Figure 9: *Electric Potential Distribution for 6-G FGM Post Type Spacer*

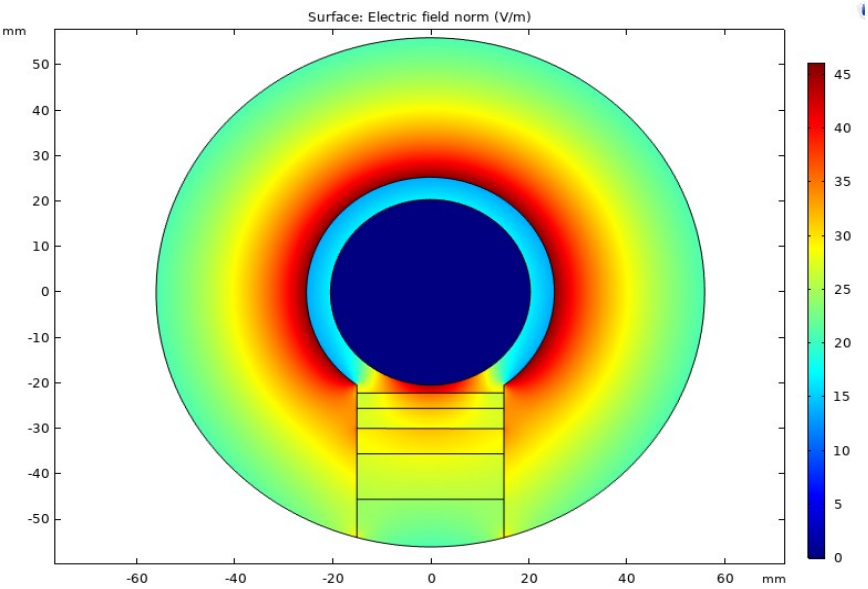

Figure 10: *Electric Field Stress Distribution Surface Plot for 6-G FGM Post Type Spacer*

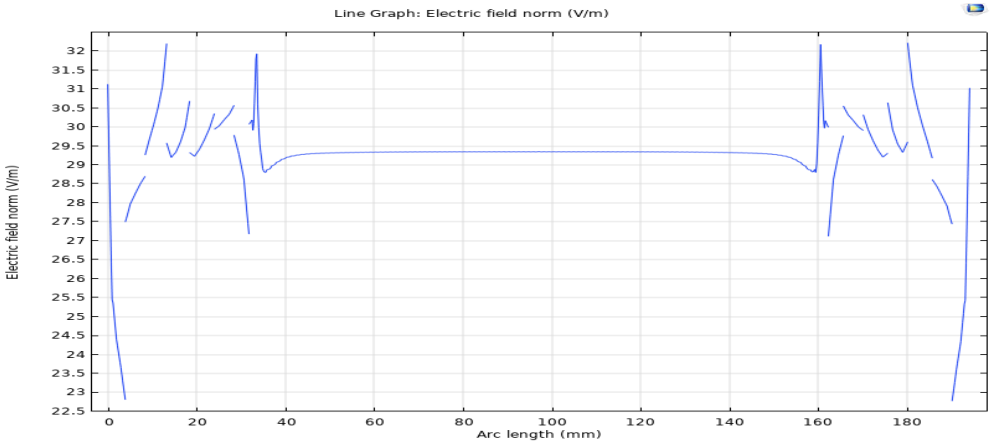

Figure 11: *Electric Field Stress Distribution Line Plot for 6G-FGM Post Type Spacer*

III. Design of 8-G FGM Spacer

The remaining two slots in the 8G-FGM spacer are subdivided to make 8 gradings in the FGM spacer as shown in Table 3. The dielectric strength of the FGM spacer is optimized for the given objective function. A sample of the optimization process is shown in Fig. 12. The optimized distribution of dielectric strength in the spacer is shown in Fig. 13.

Table 3: *Permittivity distribution in 8G-FGM Spacer*

Grading No.	Distance from the Outer enclosure (mm)	Permittivity of the FGM gradings
1	0-4.5	4.7
2	4.5-9	3.7
3	9-13.5	3.6
4	13.5-18	4.1
5	18-22.5	4.4
6	22.5-27	4.5
7	27-31.5	4.7
8	31.5-36	4

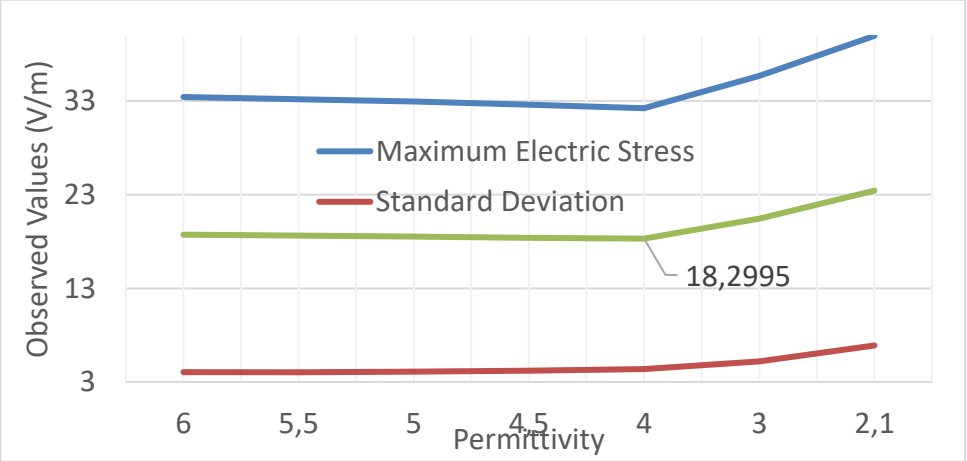

Figure 12: *Distribution of Objective function, Maximum Stress, and Standard Deviation vs permittivity for the 8th Grading of 8G-FGM Spacer*

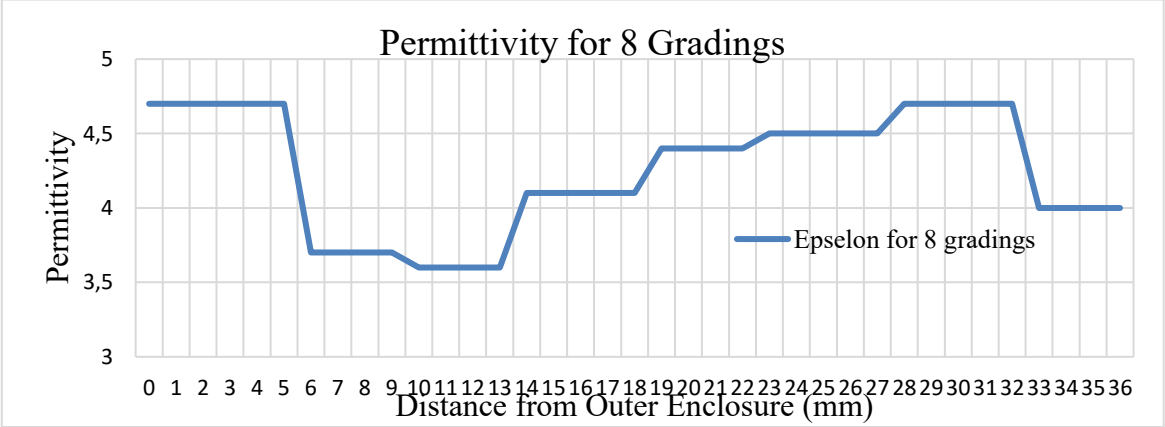

Figure 13: *Distribution of Permittivity in 8G-FGM Spacer*

The performance of the spacer is studied in terms of electric potential distribution and electric stress distribution as shown in the surface plots in Fig. 14 and Fig. 15 respectively. The line plot for electric stress vs arc length and arrow line showing the direction of the stress distribution is shown in Fig. 16 and Fig. 17 respectively. The zoomed contour plot in Fig. 18 focuses on the electric field in the stress zone. The 3D view of the electric stress distribution can be seen in Fig. 19.

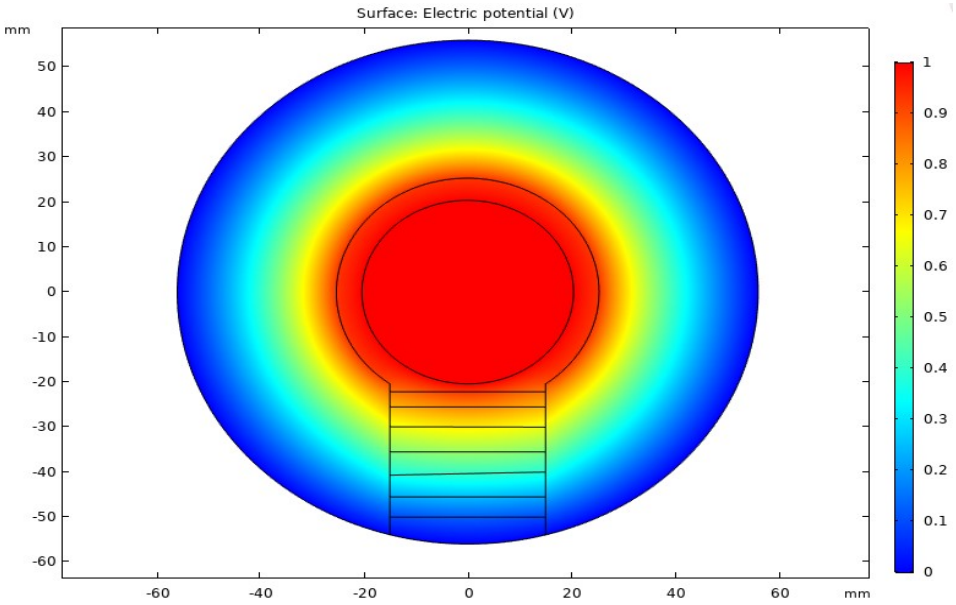

Figure 14: *Electric Field Stress Distribution Surface Plot for 8G- FGM Post Type Spacer*

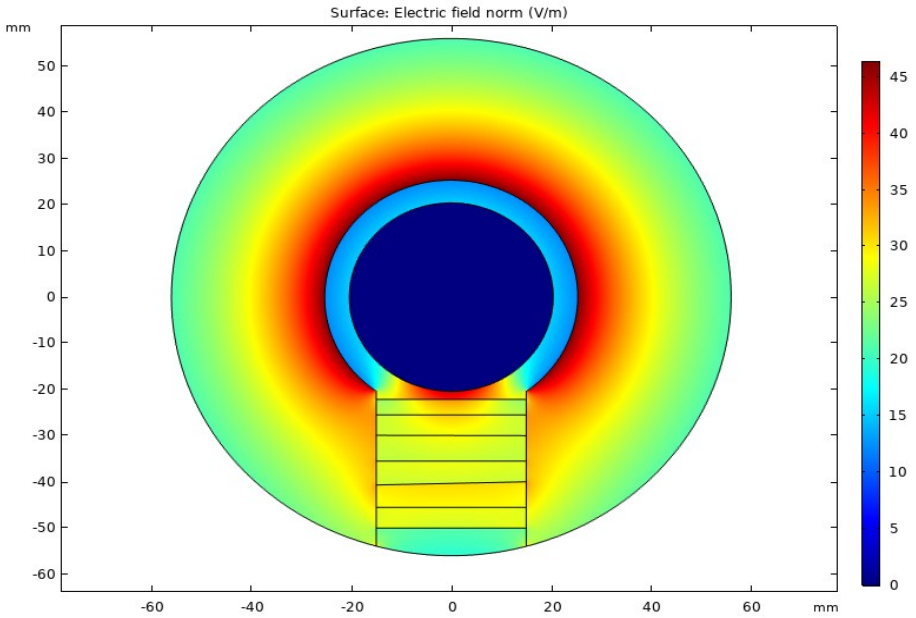

Figure 15: *Electric Potential Distribution for 6-G FGM Post Type Spacer*

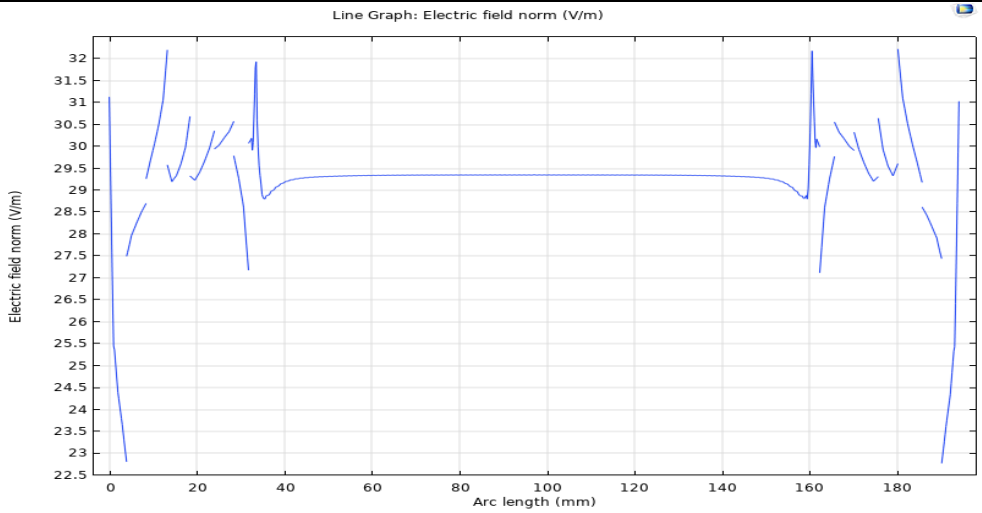

Figure 16: *Electric Field Stress Distribution Line Plot for 6-G FGM Post Type Spacer*

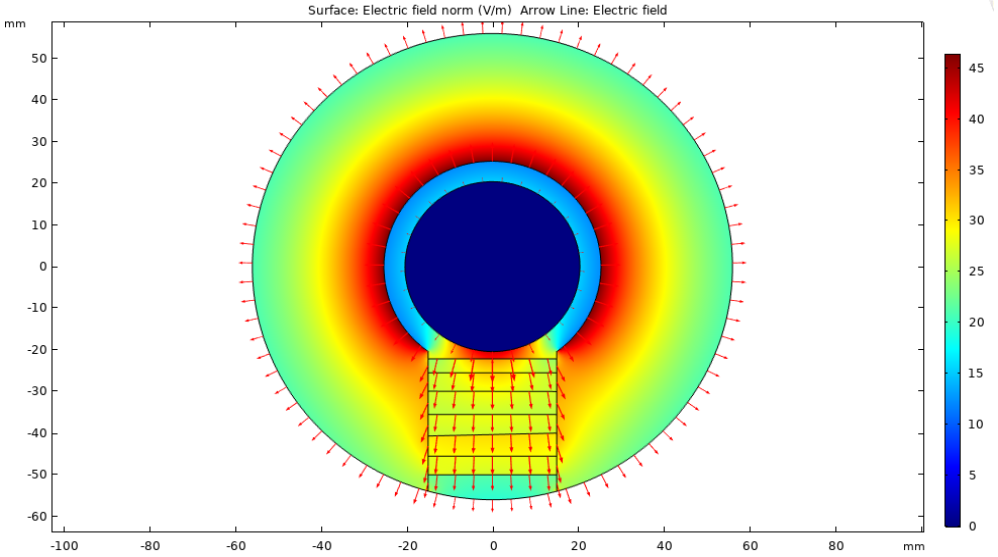

Figure 17: *Arrow line showing direction of field stress*

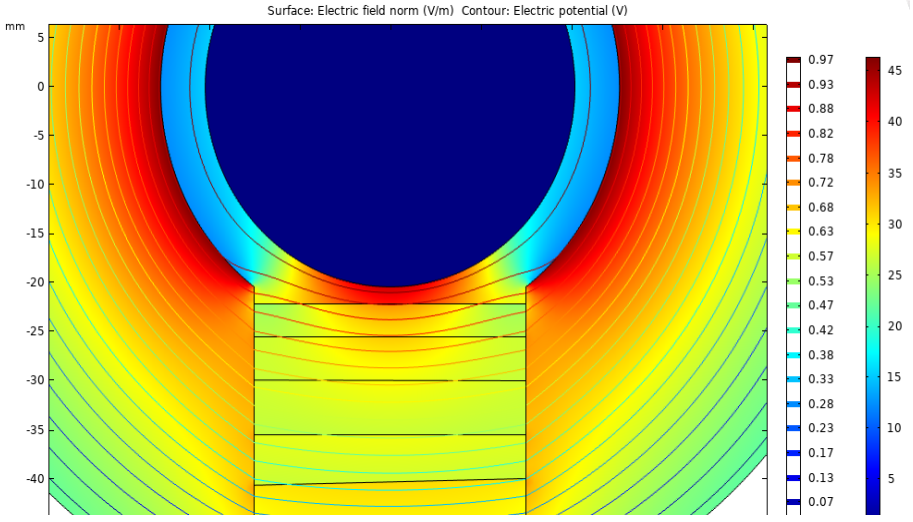

Figure 18: *Zoomed Contour Plot for Electric Stress Distribution*

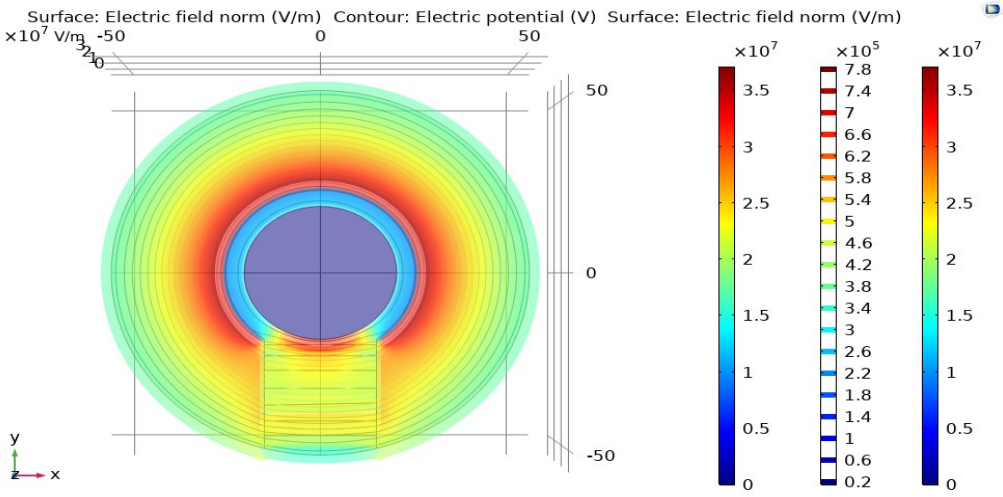

(a) XY View of electric stress distribution

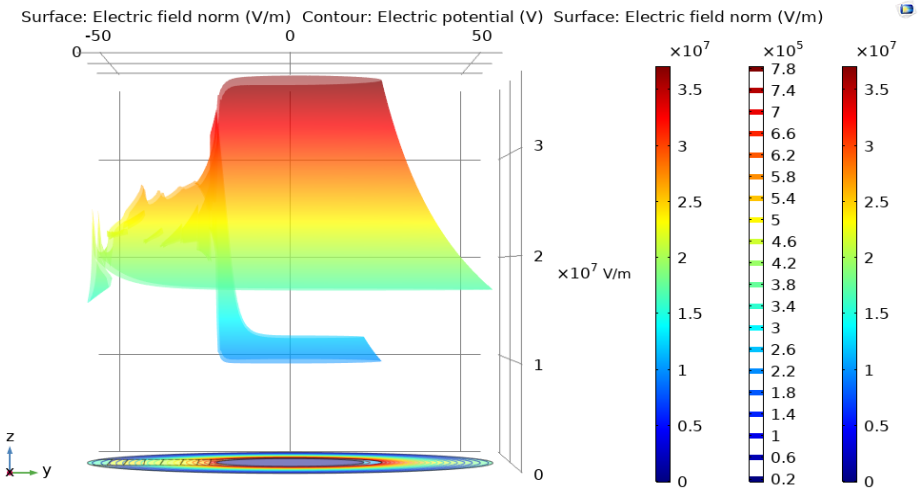

(b) YZ view of Electric Stress Distribution

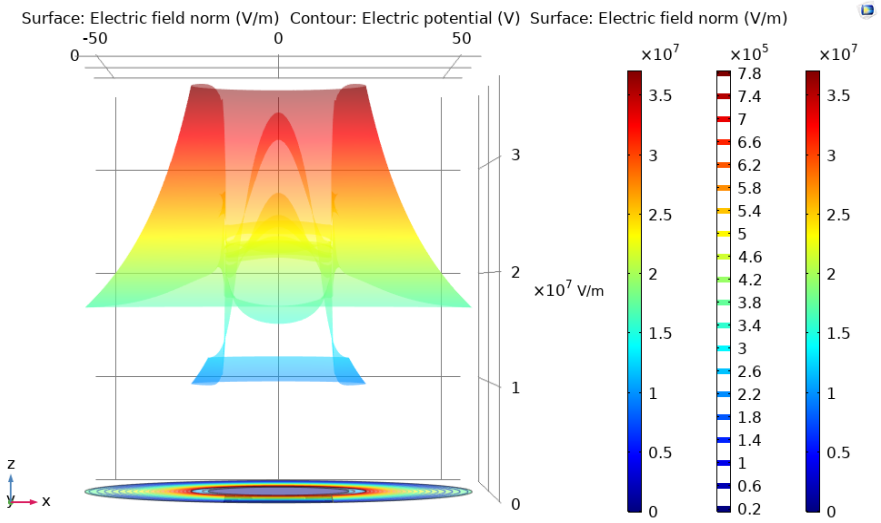

© XZ View of Electric Stress Distribution

Figure 19: *3D View of Electric Stress Distribution*

IV. Comparative Analysis of Results

A comprehensive data of the electric field distribution can be observed in Table 4 shown below. Fig. 20 shows the variation of the dielectric strength of the material in different zones for 4G-FGM, 6G-FGM and 8G-FGM respectively.

Table 4: *Distribution of dielectric strength in FGM Spacer*

Type	0 - 4.5 mm	4.5 - 9 mm	9 - 13.5 mm	13.5 – 18 mm	18 – 22.5 mm	22.5 – 27 mm	27 – 31.5 mm	31.5 – 35.5 mm
8 - Grad	4.7	3.7	3.6	4.1	4.4	4.5	4.7	4
6 - Grad	4.8		3.8		3.7	4.1	4.1	3.6
4 - Grad	4.4		4		4		4	
0 - Grad	4.1							

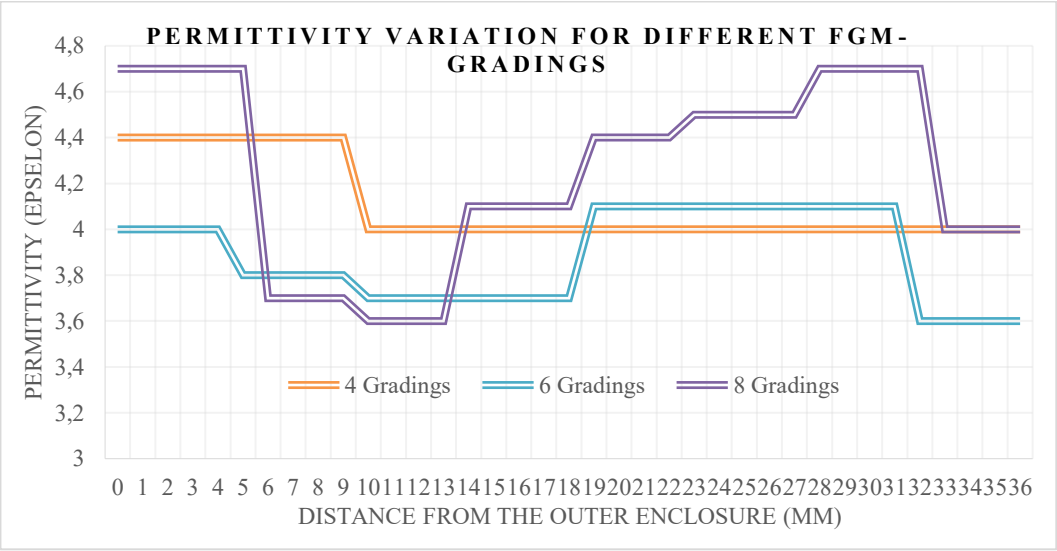

Figure 20: *Distribution of dielectric strength in the FGM-Spacer*

The comparison of the study for different gradings is presented in Table 4. Since, the average of the dielectric strength of the material in each case of FGM spacer is nearly equal to 4.1. The results obtained for different grading types are represented in Table 5. The minimum value for objective function is 18.29 which is obtained in case of 8G FGM spacer.

Table 5: *Comparison of Gradings*

S. No.	Grading Case	Maximum Electric Stress	Standard Deviation	Objective Function
1	0G; Ɛ = 4	34.4184	4.2164	19.3174
2	4G	32.3525	4.4569	18.4047
3	6G	32.7852	4.6477	18.7165
4	8G	32.2214	4.3777	18.2995

Grading high (GH), grading low (GL) and grading U (GU) are the standard methods of distribution of dielectric strength in the spacer material. The performance of the proposed design has been compared with each of the existing methods in Table 6. The distribution of the dielectric material in each of the above methods is shown in Fig. 21.

The average value of the dielectric strength in each of the cases has been maintained nearly equal to maintain uniformity.

Table 6: *Comparison with Existing Methods*

S. No.	Parameter	Proposed 8G FGM	GH-8G FGM	GL-8G FGM	GU-8G FGM
1	Maximum Electric Stress	32.2214	38.6171	35.8664	33.417
2	Standard Deviation	4.3777	4.2556	5.28	4.1066
3	Objective Function	18.2995	21.4363	20.5737	18.76

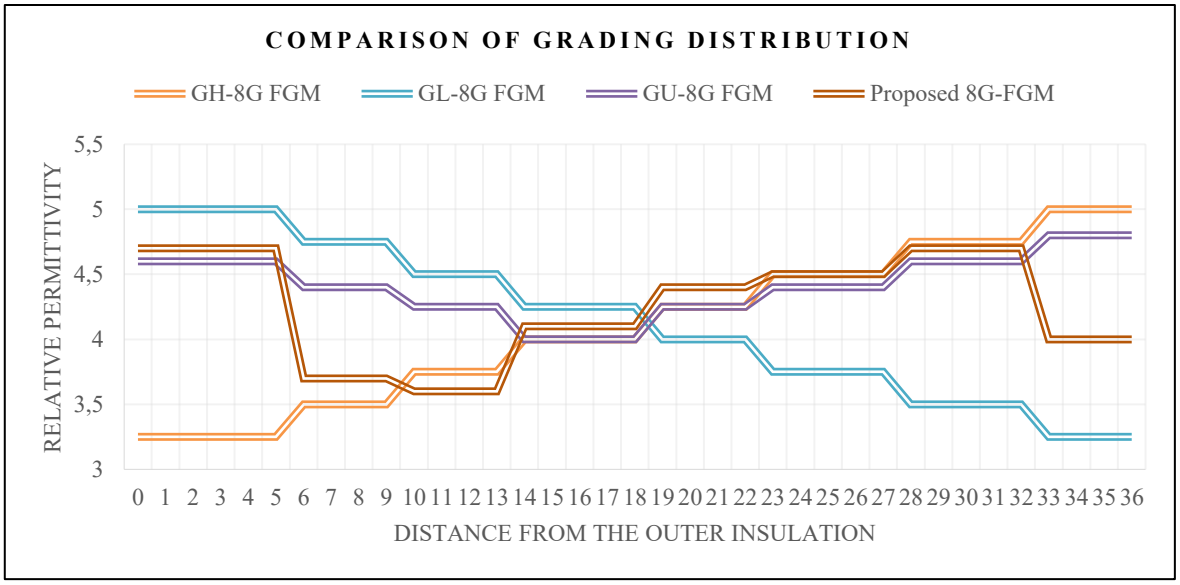

Figure 21: *Distribution of gradings in the FGM spacer for different configurations.*

V. Conclusion

An optimum design of GIS spacer can increase the reliability of the electric transmission system. In this paper, the FGM GIS spacer is designed and the results have been studied. It is observed that

- The FGM method reduces the electric stress in the spacer. There is a marked reduction in the values of the objective in FGM cases.
- The distribution of stress in the post-type spacer has been studied for each of category of FGM grading.
- All the FGM gradings have shown a satisfactory performance in reduction of the maximum electric stress and objective function. However, the 8G- FGM has been most effective in the reduction of the electric stress and the objective function.
- The comparison of the results with existing FGM methods shows that the proposed method helps to achieve a lower objective function value. Thus, the performance of the proposed FGM is better in comparison to the state of art methods.

References

[1] Feng W., Fangwei L., Lipeng Z., She C., Chuanyang L., and Yi X. (2021). Short-time X-ray Irradiation as a Non-contact Charge Dissipation Solution for Insulators in HVDC GIS/GIL, *IEEE Transactions on Dielectrics and Electrical Insulation*, 28(2): 704-709.

[2] Richard W., Moni I., Ruth H. P., Charles S. (2007). Insulated Bus Pipe (IBP) for Shipboard Applications, *IEEE Electric Ship Technologies Symposium*.8:122-129.

[3] Sridhar C., Venkatesh S. (2013). Power Loss Estimation in a 420kV Gas Insulated Busbar (GIB) by Theoretical and Simulation Techniques – A Comparison, *2013 IEEE 1st International Conference on Condition Assessment Techniques in Electrical Systems (CATCON)*, India,213-217.

[4] Uwe R. (2020). Compact High Voltage Direct Current Gas-insulated Systems, *IEEE PES Transmission and Distribution Conference and Exposition*, Chicago,1-4.

[5] Evgeni V. (2004). Dielectric Strength Coordination and Generalized Spacer Design Rules for HVAC & DC SF Gas Insulated Systems, *IEEE Transactions on Dielectrics and Electrical Insulation*, 11(6):949-963.

[6] Maria K., Karsten J., Mark K., Dejun L, (2019). Overview of development, design, testing and application of compact gas-insulated DC systems up to ±550 kV, *Global Energy Interconnection*, 2(6): 567-577.

[7] Boxue D., Jin L. and Hucheng L.(2019). Electrical Field Distribution along HVDC GIL Spacer in SF6/N2 Gaseous Mixture, *Electric Power Conversion*, 1-19.

[8] Sayed A. W., Turky G.M., Shabayek D. M. (2014). Electric Field Stress Calculation for different spacer types in Bus Duct, *International Journal of Scientific Research Engineering & Technology (IJSRET)*, 3(6): 958-963.

[9] C. Li, B. Liu, J. Wang, R. Gong etal(2019). Novel HVDC Spacers in GIS/GIL by Adaptively Controlling Surface Charges – Insulation Compounding Scheme, *2nd International Conference on High Voltage Engineering and Power Systems (ICHVEPS),* Indonesia,38-44.

[10] Zhang B., Zhong J., Han G. (2020). Modification of HVDC GIS/GIL Basin Insulators Based on Electrical and Mechanical Collaborative Design, *2020 IEEE International Conference on High Voltage Engineering and Application (ICHVE)*, China, 1-5.

[11] Syarif H., Fransiskus D., Umar K. (2016). Electric Field Optimization on 150 kV GIS Spacer using Functionally Gradient Material, *2nd International Conference of Industrial, Mechanical, Electrical, Chemical Engineering (ICIMECE),*Indonesia, 254-259.

[12] Abd Allah M. A., Sayed A. W., Youssef A. A. (2013) Effect of Functionally Graded Material of Disc Spacer with Presence of Multi-Contaminating Particles on Electric Field inside Gas Insulated Bus Duct, *International Journal of Electrical and Computer Engineering (IJECE)*, 3(6): 831-848.

[13] Muneaki K., Masahiro H., Hitoshi O. (2010). Application of Functionally Graded Material for Reducing Electric Field on Electrode and Spacer Interface, *IEEE Transactions on Dielectrics and Electrical Insulation*, 17(1):256-263.

[14] Jagadeesh A., Venkata Siva Krishna R. G., Venkata Nagesh Kumar G. (2018). Mitigation of field stress with metal inserts for cone type spacer in a gas insulated busduct under delamination, *Engineering Science and Technology*, 21(5): 850–861.

[15] Janaki P., Karthick N. & Nagesh Kumar G. V., (2020). Study of electrostatic field effect in a three-phase gas-insulated busduct with FGM spacer under the effect of protrusion, *Journal of Electromagnetic Waves and Applications*, 34(16): 2107–2129.

[16] Janaki P., Nagesh Kumar G. V., Deepak Chowdary D., Sravana Kumar B.(2020). Study of electric field stress on the surface contour and at the triple junction in three phase GIS with FGM spacer under the depression defect, *International Journal of Emerging Electric Power Systems*, 21(5):20200080.

[17] Gopichand Naik M., Amarnath J., and Kamakshiah S.,(2012) Computation of Electric Field for FGM Spacer Using Di-Post Insulator in GIS, *International Journal of Electrical Engineering*, 5(4): 465-474.

[18] Metwally I. A., (2012). Reduction of electric-field intensification inside GIS by controlling spacer material and design, *Journal of Electrostatics*, 70(2): 217-224.

[19] Syed Abdullah Q. and Nandini G. (2015). Use of Particle Swarm Optimization in the Computation of an optimal permittivity distribution in Functionally Graded Material insulators, *International Conference on Condition Assessment Techniques in Electrical Systems (CATCON),* India, 184-188.

[20] Talaata M., El-Zein A., Amin M. (2017). Developed optimization technique used for the distribution of U-shaped permittivity for cone type spacer in GIS, *Electric Power Systems Research,* 163:754-766.

[21] William H. Hayt Jr., Engineering Electromagnetics, fifth ed., McGraw-Hill Book Company, 1989.